
A NEURAL NETWORK BASED ON-DEVICE LEARNING ANOMALY DETECTOR FOR EDGE DEVICES

A PREPRINT

Mineto Tsukada

Keio University
3-14-1 Hiyoshi, Kohoku-ku, Yokohama, Japan
tsukada@arc.ics.keio.ac.jp

Masaaki Kondo

The University of Tokyo
7-3-1 Hongo, Bunkyo-ku, Tokyo, Japan
kondo@hal.ipc.i.u-tokyo.ac.jp

Hiroki Matsutani

Keio University
3-14-1 Hiyoshi, Kohoku-ku, Yokohama, Japan
matutani@arc.ics.keio.ac.jp

July 25, 2019

ABSTRACT

Semi-supervised anomaly detection is referred as an approach to identify rare data instances (i.e., anomalies) on the assumption that all the available training data belong to the majority (i.e., the normal class). A typical strategy is to model distributions of normal data, then identify data samples far from the distributions as anomalies. Nowadays, backpropagation based neural networks (i.e., BP-NNs) have been drawing attention as well as in the field of semi-supervised anomaly detection because of their high generalization capability for real-world high dimensional data. As a typical application, such BP-NN based models are iteratively optimized in server machines with accumulated data gathered from edge devices such as smartphones, surveillance cameras, self-driving cars, smart speakers, etc. However, there are two issues in this framework: (1) BP-NNs' iterative optimization approach often takes too long time to follow changes of the distributions of normal data (i.e., concept drift), and (2) data transfers between servers and edge devices have a potential risk to cause data breaches. To address these underlying issues, we propose an ON-device sequential Learning semi-supervised Anomaly Detector called ONLAD. The aim of this work is to propose the algorithm, and also to implement it as an IP core called ONLAD Core so that various kinds of edge devices can adopt our approach at low power consumption. Experimental results using open datasets show that ONLAD has favorable anomaly detection capability especially in a testbed which simulates concept drift. Experimental results on hardware performance of the FPGA based ONLAD Core show that its training latency and prediction latency are $\times 1.95$ - $\times 4.51$ and $\times 2.29$ - $\times 4.73$ faster than those of BP-NN based software implementations. It is also confirmed that our on-board implementation of ONLAD Core actually works at $\times 6.7$ - $\times 27.1$ lower power consumption than the other software implementations at a high workload.

Keywords On-device Learning · Neural Networks · Semi-supervised Anomaly Detection · OS-ELM · FPGA

1 Introduction

Anomaly detection is referred as an approach to identify rare data instances (i.e., anomalies) which have different patterns or come from a different distribution from the majority (i.e., the normal class) [1]. There are mainly three types of anomaly detection approaches: (1) supervised anomaly detection, (2) semi-supervised anomaly detection, and (3) unsupervised anomaly detection. Among them, (2) and (3) especially do not require anomalies for training models, which makes them more widely applicable to real-world problems. In this work, we focus on semi-supervised

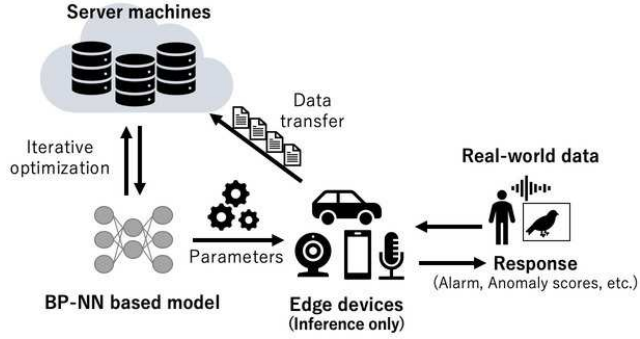


Figure 1: A typical application of BP-NN based semi-supervised anomaly detection models

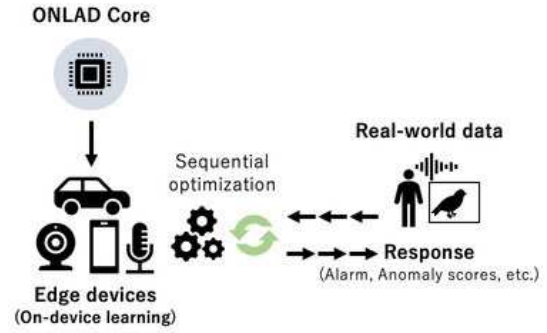


Figure 2: On-device sequential learning approach

anomaly detection. Semi-supervised anomaly detection assumes all the training data belong to the normal class. A typical strategy of semi-supervised methods is to model distributions of normal data, then identify data samples distant from the distributions as anomalies.

Various types of semi-supervised methods, such as Gaussian Mixture Model [2] based techniques, Naïve Bayes based techniques, K-NN [3] based techniques, PCA [4] based techniques, and One-Class SVM [5] based techniques have been proposed so far. Nowadays, neural network based approaches [6, 7, 8] have been drawing attention because in many cases they have relatively higher generalization capability than traditional methods for high dimensional data such as images, natural languages, and audio data. There are several types of neural networks proposed so far, though currently backpropagation based neural networks (i.e., BP-NNs) are especially widely used.

Figure 1 shows one of typical applications using BP-NN based semi-supervised anomaly detection models. Suppose there are a cluster of server machines and edge devices (e.g., smartphones, surveillance cameras, self-driving cars, smart speakers, etc) which take a role as the entrance of real-world data. Typically, the edge devices transfer input data to the server machines, then the models are iteratively trained with the accumulated data in the server machines. Once the training loop completes, the optimized parameters are transferred to the edge devices. However, there are two issues in the system: (1) BP-NNs’ iterative optimization approach often takes a long time to achieve high generalization capability, and (2) data transfers between servers and edge devices have a potential risk to cause data breaches.

(1) As mentioned before, it is a key feature for semi-supervised anomaly detection methods to model distributions of normal data. However, the distributions can dynamically change in time-series. The phenomenon is referred as concept drift [9]. It often becomes a severe problem due to dynamical changes of surrounding environment [9] or behavioral state transition of the target objects or users [10]. It is important to follow the changes as soon as possible, though BP-NN’s iterative optimization approach often takes a long time; basically BP-NNs have to be iteratively trained with a large amount of accumulated data to achieve high generalization capability. The delay widens the gap between the latest true distributions of normal data and ones trained by the models [11], which makes identifying anomalies more difficult. To address this issue, the iterative optimization approach should be replaced with another approach which is able to perform fast sequential training where each data sample is sequentially learned in one-step.

(2) In many cases, edge devices are specialized only for prediction computations because backpropagation optimization often requires a large computational capability, therefore training tasks are typically offloaded to server machines. For this reason, data transfers between edge devices and server machines are inevitable.

One practical solution for the issues is the on-device sequential learning approach illustrated in Figure 2. In this framework, edge devices themselves sequentially learn each data sample in one-shot. This approach allows to immediately follow changes of distributions of normal data, and realizes standalone execution where no data transfer is assumed. However, there are some challenges to realize the approach: how to construct such a sequential learning algorithm, then how to implement the algorithm on edge devices where only limited resources are available.

Our proposed approach, an ON-device sequential Learning semi-supervised Anomaly Detector called ONLAD, deals with the underlying challenges. The aim of this work is to propose the algorithm, and also to implement it as an IP core (ONLAD Core illustrated in Figure 2) so that various kinds of edge devices can adopt our approach at low power consumption¹. We make the following four contributions in this work:

¹ This work is an extended version of our prior work [12] by adding a forgetting mechanism and thorough experimental results.

1. ONLAD utilizes OS-ELM [13], a lightweight neural network which is able to perform fast sequential learning, as the core component. In Section 3.1, we provide a theoretical analysis on the computational complexity of OS-ELM. We demonstrate that the computational cost of the training algorithm is significantly reduced with no deterioration of training results when batch size of OS-ELM is equal to 1.
2. In Section 3.2, we propose a low-cost forgetting mechanism for OS-ELM. As mentioned before, a key factor for semi-supervised anomaly detection models is to correctly model distributions of normal data, though they can change in time-series. In case of that, it is desired that OS-ELM, the core component of ONLAD, is able to analytically forget the past distributions of normal data to follow the new ones. The proposed forgetting mechanism provides such a feature for OS-ELM with low computational cost.
3. In Section 3.3, we propose ONLAD, a new sequential learning semi-supervised anomaly detection algorithm which constructs an OS-ELM based autoencoder. Autoencoder [14] is originally proposed as a neural network based unsupervised learning model, though it also has been attracted attention as a semi-supervised anomaly detection model. The combination of Autoencoder and OS-ELM, and the proposed techniques for reducing computational cost realizes fast sequential learning semi-supervised anomaly detection on resource-limited edge devices. Also, anomaly detection capability of ONLAD is evaluated with open datasets in Section 5.
4. In Section 4, we propose an FPGA based design and implementation of ONLAD Core. We also evaluate the FPGA based ONLAD Core in terms of training/prediction latency, FPGA resource utilization, and on-board power consumption in Section 6.

The rest of this paper is organized as follows: Section 2 provides a brief review of basic technologies behind ONLAD. We propose ONLAD in Section 3. Section 4 describes the FPGA based design and implementation of ONLAD Core. ONLAD is evaluated in terms of anomaly detection capability in Section 5, then the FPGA based implementation is also evaluated in terms of hardware performance in Section 6. Finally, Section 7 concludes this paper.

2 Preliminaries

This section provides a brief introduction of base technologies behind ONLAD: (1) ELM (Extreme Learning Machine), (2) OS-ELM (Online Sequential Extreme Learning Machine), and (3) Autoencoder.

2.1 ELM

ELM [15] shown in Figure 3 is a single hidden layer feedforward network (i.e., SLFN) which consists of an input layer, a hidden layer, and an output layer. Suppose an n -dimensional input chunk $\mathbf{x} \in \mathbf{R}^{k \times n}$ of batch size k is given, an m -dimensional output chunk $\mathbf{y} \in \mathbf{R}^{k \times m}$ is computed as follows.

$$\mathbf{y} = G(\mathbf{x} \cdot \boldsymbol{\alpha} + \mathbf{b})\boldsymbol{\beta}, \tag{1}$$

where $\boldsymbol{\alpha} \in \mathbf{R}^{n \times \tilde{N}}$ is an input weight connecting the input layer and the hidden layer, and $\boldsymbol{\beta} \in \mathbf{R}^{\tilde{N} \times m}$ is an output weight connecting the hidden layer and the output layer. $\mathbf{b} \in \mathbf{R}^{\tilde{N}}$ is a bias vector of the hidden layer, and G denotes an activation function applied to the hidden layer output.

If a SLFN model can approximate m -dimensional target chunk $\mathbf{t} \in \mathbf{R}^{k \times m}$ with zero error, it implies that there exists $\boldsymbol{\beta}$ that satisfies the following equation.

$$G(\mathbf{x} \cdot \boldsymbol{\alpha} + \mathbf{b})\boldsymbol{\beta} = \mathbf{t} \tag{2}$$

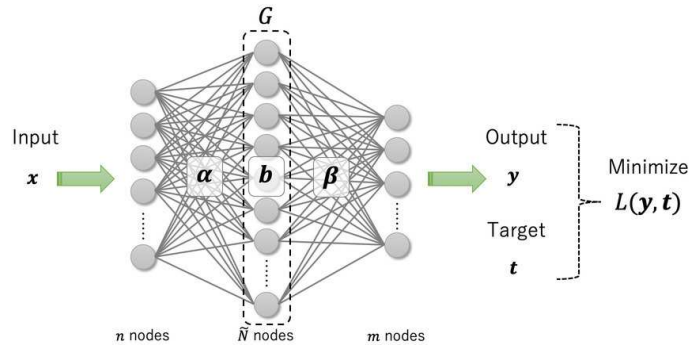


Figure 3: Extreme Learning Machine

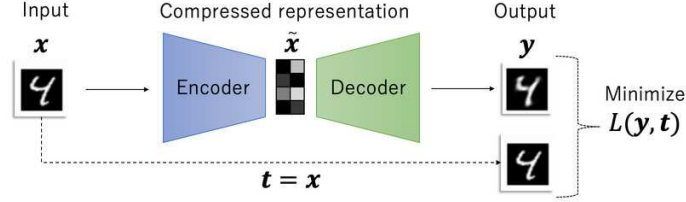


Figure 4: Autoencoder

Let $\mathbf{H} \in \mathbf{R}^{k \times \tilde{N}}$ be the hidden layer output $G(\mathbf{x} \cdot \boldsymbol{\alpha} + \mathbf{b})$, then the optimal output weight is computed as follows.

$$\hat{\boldsymbol{\beta}} = \mathbf{H}^\dagger \mathbf{t}, \quad (3)$$

where \mathbf{H}^\dagger is the pseudo inverse of \mathbf{H} . It can be calculated with matrix decomposition algorithms such as SVD (Singular Value Decomposition) [16]. The whole training process completes by just replacing $\boldsymbol{\beta}$ with $\hat{\boldsymbol{\beta}}$.

Although BP-NNs have to train both $\boldsymbol{\alpha}$ and $\boldsymbol{\beta}$, ELM computes only the optimal solution of $\boldsymbol{\beta}$ ($\boldsymbol{\alpha}$ does not change once initialized with random values). That saves computational cost to optimize $\boldsymbol{\alpha}$. In addition to that, ELM's training is not an iterative optimization method unlike BP-NNs but a one-shot optimization approach, which makes the whole training process faster. It is known that ELM can compute the optimal output weight faster than BP-NNs [15].

Please note that ELM is categorized as one of batch learning algorithms where all the training samples are assumed to be available in advance, which means retraining for the whole dataset is needed to learn new training samples.

2.2 OS-ELM

OS-ELM [13] is an ELM based algorithm extended to be able to perform sequential learning instead of batch learning. Suppose the i th training chunk $\{\mathbf{x}_i \in \mathbf{R}^{k_i \times n}, \mathbf{t}_i \in \mathbf{R}^{k_i \times m}\}$ of batch size k_i is given, we need to find $\boldsymbol{\beta}$ which minimizes the following error.

$$\left\| \begin{bmatrix} \mathbf{H}_0 \\ \vdots \\ \mathbf{H}_i \end{bmatrix} \boldsymbol{\beta}_i - \begin{bmatrix} \mathbf{t}_0 \\ \vdots \\ \mathbf{t}_i \end{bmatrix} \right\|, \quad (4)$$

where \mathbf{H}_i is defined as $\mathbf{H}_i \equiv G(\mathbf{x}_i \cdot \boldsymbol{\alpha} + \mathbf{b})$. The optimal output weight is then computed as follows.

$$\begin{aligned} \mathbf{P}_i &= \mathbf{P}_{i-1} - \mathbf{P}_{i-1} \mathbf{H}_i^T (\mathbf{I} + \mathbf{H}_i \mathbf{P}_{i-1} \mathbf{H}_i^T)^{-1} \mathbf{H}_i \mathbf{P}_{i-1} \\ \boldsymbol{\beta}_i &= \boldsymbol{\beta}_{i-1} + \mathbf{P}_i \mathbf{H}_i^T (\mathbf{t}_i - \mathbf{H}_i \boldsymbol{\beta}_{i-1}) \end{aligned} \quad (5)$$

Especially, \mathbf{P}_0 and $\boldsymbol{\beta}_0$ are computed as follows.

$$\begin{aligned} \mathbf{P}_0 &= (\mathbf{H}_0^T \mathbf{H}_0)^{-1} \\ \boldsymbol{\beta}_0 &= \mathbf{P}_0 \mathbf{H}_0^T \mathbf{t}_0 \end{aligned} \quad (6)$$

As shown in Equation 5, OS-ELM can sequentially find the optimal output weight in one-shot for the new training chunk without memory or retraining for past training samples unlike ELM. OS-ELM still can find the optimal solution faster than BP-NNs [13].

2.3 Autoencoder Based Semi-Supervised Anomaly Detection

Autoencoder [14] shown in Figure 4 is a neural network based unsupervised learning model for finding a well-characterized dimensionally reduced form $\tilde{\mathbf{x}} \in \mathbf{R}^{k \times \tilde{n}}$ of an input chunk $\mathbf{x} \in \mathbf{R}^{k \times n}$ ($\tilde{n} < n$). In general, output of an intermediate layer is regarded as $\tilde{\mathbf{x}}$. Especially a SLFN model including ELM and OS-ELM has only one intermediate layer, therefore the hidden layer output \mathbf{H} is regarded as $\tilde{\mathbf{x}}$. Basically, the number of hidden nodes \tilde{n} is constrained to be less than that of input nodes n . In this case, such autoencoders are especially referred as **undercomplete autoencoders**. In the case of the opposite setting (i.e., $n < \tilde{n}$), such autoencoders are especially referred as **overcomplete autoencoders**. Although overcomplete autoencoders cannot perform dimensionally reduction, it is known that they can obtain well-characterized representations for classification problems by applying regularization conditions or noise [17] to the loss function.

In the training process, all the input samples are also used as their targets (i.e., $\mathbf{t} = \mathbf{x}$), therefore an autoencoder is trained so as to reconstruct input samples in output as correctly as possible. It is known that $\tilde{\mathbf{x}}$ tends to become

well-characterized when the error between \boldsymbol{x} and the reconstructed output converges [14]. Please note that any labeled data are not required during the whole training process; this is why Autoencoder is categorized as an unsupervised learning method.

Autoencoder also has attracted attention as a semi-supervised anomaly detection model [7, 18]. In this context, an autoencoder is trained only with normal data. Then, the autoencoder becomes to output relatively high reconstruction errors for anomalies. Thus, anomalies can be detected by setting a threshold for reconstruction errors. Please note that this approach is categorized as a semi-supervised anomaly detection method since only normal data are used for training models.

PCA (Principal Component Analysis), another non-statistical dimensionally reduction algorithm which is also used as a semi-supervised anomaly detection model, is often mentioned as a similar approach to Autoencoder. Sakurada *et al.* showed that autoencoder based models can detect subtle anomalies which PCA fails to detect [7]. Moreover, autoencoder based models can apply nonlinear transformation without costly computations which kernel PCA [19] requires.

3 ONLAD

As mentioned in the introduction, our ONLAD utilizes OS-ELM as the core component. In this section, we firstly provide a theoretical analysis of OS-ELM and demonstrate that the computational cost of the training algorithm is significantly reduced when batch size = 1 without any deterioration of training results. We also propose a computationally lightweight forgetting mechanism for OS-ELM. It allows ONLAD to gradually forget past training data with a controllable parameter to deal with concept drift with low computational cost. Finally, the algorithm of ONLAD is formulated.

3.1 Analysis of OS-ELM

The training algorithm of OS-ELM (i.e., Equation 5) mainly consists of the following two matrix operations: (1) matrix product and (2) matrix inversion. Suppose the computational iterations for a matrix product $\boldsymbol{A} \in \mathbf{R}^{p \times q} \cdot \boldsymbol{B} \in \mathbf{R}^{q \times r}$ is pqr , and that for a matrix inversion $\boldsymbol{C}^{-1} \in \mathbf{R}^{r \times r}$ is r^3 , then the total computational iterations for these two operations in Equation 5 is calculated as follows.

$$\begin{aligned} I_{prod} &= 4k\tilde{N}^2 + k(2k + 2m + n)\tilde{N} \\ I_{inv} &= k^3, \end{aligned} \tag{7}$$

where I_{prod} is the total computational iterations for matrix products, while I_{inv} denotes that for matrix inversions. n , \tilde{N} , and m are the numbers of input, hidden, and output nodes of OS-ELM, respectively. k denotes batch size. For example, the computational iterations for $\boldsymbol{H}_i \boldsymbol{P}_{i-1} \boldsymbol{H}_i^T$ is calculated by dividing the computing process into the following two steps: (1) $\boldsymbol{H}_i \in \mathbf{R}^{k \times \tilde{N}} \cdot \boldsymbol{P}_{i-1} \in \mathbf{R}^{\tilde{N} \times \tilde{N}}$ and (2) $\boldsymbol{H}_i \boldsymbol{P}_{i-1} \in \mathbf{R}^{k \times \tilde{N}} \cdot \boldsymbol{H}_i^T \in \mathbf{R}^{\tilde{N} \times k}$. In this case, these computational iterations are calculated as $k\tilde{N}^2$ and $k^2\tilde{N}$, respectively.

Let I_k be the total computational iterations for matrix products and matrix inversions in Equation 5 when batch size = k , then we can derive the following equation.

$$\begin{aligned} I_k &= I_{prod} + I_{inv} \\ &= 4k\tilde{N}^2 + k(2k + 2m + n)\tilde{N} + k^3 \\ &= k(4\tilde{N}^2 + (2k + 2m + n)\tilde{N} + k^2) \\ &\geq k(4\tilde{N}^2 + (2 + 2m + n)\tilde{N} + 1) = kI_1 \end{aligned} \tag{8}$$

Finally $I_k \geq kI_1$ is obtained. This inequality shows that the training algorithm becomes computationally more efficient when batch size = 1 than batch size = k . Please note that the insight does not always make sense for software implementations because software-specific overheads such as memory allocation or function calls should be taken into account. However, baremetal implementations, including ONLAD Core, can fully enjoy the insight since they are free from any kinds of these overheads. Moreover, when $k = 1$, the computational cost of the matrix inversion $(\boldsymbol{I} + \boldsymbol{H}_i \boldsymbol{P}_{i-1} \boldsymbol{H}_i^T)^{-1}$ in Equation 5 is significantly reduced as the size of the target matrix $\boldsymbol{I} + \boldsymbol{H}_i \boldsymbol{P}_{i-1} \boldsymbol{H}_i^T$ is $k \times k$. In this case, the following training algorithm is derived from Equation 5.

$$\begin{aligned} \boldsymbol{P}_i &= \boldsymbol{P}_{i-1} - \frac{\boldsymbol{P}_{i-1} \boldsymbol{h}_i^T \boldsymbol{h}_i \boldsymbol{P}_{i-1}}{1 + \boldsymbol{h}_i \boldsymbol{P}_{i-1} \boldsymbol{h}_i^T} \\ \boldsymbol{\beta}_i &= \boldsymbol{\beta}_{i-1} + \boldsymbol{P}_i \boldsymbol{h}_i^T (\boldsymbol{t}_i - \boldsymbol{h}_i \boldsymbol{\beta}_{i-1}), \end{aligned} \tag{9}$$

where $\mathbf{h} \in \mathbf{R}^{\tilde{N}}$ denotes a special case of $\mathbf{H} \in \mathbf{R}^{k \times \tilde{N}}$ when $k = 1$. Thanks to the trick, ONLAD can perform training without any costly matrix inversions. That helps to reduce not only the computational cost but also the amount of hardware resources of ONLAD Core. That also makes easier to parallelize the training algorithm because now there are no matrix operations of low degree of parallelism such as matrix inversion.

Furthermore, training results of OS-ELM do not get affected even if batch size = 1 because OS-ELM gives exactly the same output weight when training N times with batch size = k , or when training Nk times with batch size = 1. This is a notable difference from BP-NNs; they are usually trained with batch size $k \gg 1$ to maintain stable convergence during training process and to get better generalization capability. Based on the above discussion, the batch size of OS-ELM used in ONLAD is always fixed to 1.

3.2 Lightweight Forgetting Mechanism for OS-ELM

In some real environments, distributions of normal data can change as time goes by. In this case, it is desired that ONLAD has a functionality to forget past learned data with a controllable parameter, and of course even it should be executed with low computational cost. To deal with the challenge, we propose a computationally lightweight forgetting mechanism based on FP-ELM (Forgetting Parameters Extreme Learning Machine) [20], one of the state-of-the-art forgetting mechanisms for OS-ELM.

3.2.1 Review of FP-ELM

This section provides a brief review of FP-ELM. The training algorithm of FP-ELM is formulated as follows.

$$\begin{aligned} \mathbf{K}_i &= \alpha_i^2 \mathbf{K}_{i-1} + \mathbf{H}_i^T \mathbf{H}_i \\ \boldsymbol{\beta}_i &= \boldsymbol{\beta}_{i-1} + (\lambda \mathbf{I} + \mathbf{K}_i)^{-1} (\mathbf{H}_i^T (\mathbf{t}_i - \mathbf{H}_i \boldsymbol{\beta}_{i-1}) - \lambda (1 - \alpha_i^2) \boldsymbol{\beta}_{i-1}) \end{aligned} \quad (10)$$

Especially, \mathbf{K}_0 and $\boldsymbol{\beta}_0$ are computed as follows.

$$\begin{aligned} \mathbf{K}_0 &= \mathbf{H}_0^T \mathbf{H}_0 \\ \boldsymbol{\beta}_0 &= (\lambda \mathbf{I} + \mathbf{H}_0^T \mathbf{H}_0)^{-1} \mathbf{H}_0^T \mathbf{t}_0, \end{aligned} \quad (11)$$

where λ is the L2 regularization parameter for $\boldsymbol{\beta}$. This parameter limits the L2 norm $\|\boldsymbol{\beta}\|$ so that it does not become too large to prevent overfitting. α_i ($0 \leq \alpha_i \leq 1$) is the forgetting parameter which controls the weight (i.e., the significance) of each past training chunk. Suppose the latest training step is i , then w_k , the weight of the k th training chunk, is gradually decayed at every step as shown below.

$$w_k = \begin{cases} \prod_{j=k+1}^i \alpha_j, & (0 \leq k \leq i-1) \\ 1, & (k = i) \end{cases} \quad (12)$$

Please note that α_i is a variable parameter, which enables to adaptively control progress of forgetting.

3.2.2 Proposed Forgetting Mechanism

FP-ELM can analytically control the weights of past training chunks. However, FP-ELM cannot remove the matrix inversion $(\lambda \mathbf{I} + \mathbf{P}_i)^{-1}$ in Equation 10 even if batch size = 1 because the size of $\lambda \mathbf{I} + \mathbf{P}_i$ is $\tilde{N} \times \tilde{N}$ where \tilde{N} denotes the number of hidden nodes. In order to address the issue, we modify FP-ELM so that it can remove the matrix inversion when batch size = 1.

Firstly, the following equations are derived by disabling the L2 regularization trick (i.e., let $\lambda = 0$) in Equation 10.

$$\begin{aligned} \mathbf{K}_i &= \alpha_i^2 \mathbf{K}_{i-1} + \mathbf{H}_i^T \mathbf{H}_i \\ \boldsymbol{\beta}_i &= \boldsymbol{\beta}_{i-1} + \mathbf{K}_i^{-1} \mathbf{H}_i^T (\mathbf{t}_i - \mathbf{H}_i \boldsymbol{\beta}_{i-1}) \end{aligned} \quad (13)$$

The update formula of \mathbf{K}_i^{-1} is also derived with the Woodbury formula [21]².

$$\begin{aligned} \mathbf{K}_i^{-1} &= (\alpha_i^2 \mathbf{K}_{i-1} + \mathbf{H}_i^T \mathbf{H}_i)^{-1} \\ &= \left(\frac{1}{\alpha_i^2} \mathbf{K}_{i-1} \right) - \left(\frac{1}{\alpha_i^2} \mathbf{K}_{i-1} \right) \mathbf{H}_i^T \left(\mathbf{I} + \mathbf{H}_i \left(\frac{1}{\alpha_i^2} \mathbf{K}_{i-1} \right) \mathbf{H}_i^T \right)^{-1} \mathbf{H}_i \left(\frac{1}{\alpha_i^2} \mathbf{K}_{i-1} \right) \end{aligned} \quad (14)$$

² $(\mathbf{A} + \mathbf{UCV})^{-1} = \mathbf{A}^{-1} - \mathbf{A}^{-1} \mathbf{U} (\mathbf{C}^{-1} + \mathbf{VA}^{-1} \mathbf{U})^{-1} \mathbf{VA}^{-1}$

Finally, the training algorithm is obtained by defining \mathbf{P}_i as $\mathbf{P}_i \equiv \mathbf{K}_i^{-1}$.

$$\begin{aligned}\mathbf{P}_i &= \left(\frac{1}{\alpha_i^2} \mathbf{P}_{i-1}\right) - \left(\frac{1}{\alpha_i^2} \mathbf{P}_{i-1}\right) \mathbf{H}_i^T (\mathbf{I} + \mathbf{H}_i \left(\frac{1}{\alpha_i^2} \mathbf{P}_{i-1}\right) \mathbf{H}_i^T)^{-1} \mathbf{H}_i \left(\frac{1}{\alpha_i^2} \mathbf{P}_{i-1}\right) \\ \boldsymbol{\beta}_i &= \boldsymbol{\beta}_{i-1} + \mathbf{P}_i \mathbf{H}_i^T (\mathbf{t}_i - \mathbf{H}_i \boldsymbol{\beta}_{i-1})\end{aligned}\quad (15)$$

\mathbf{P}_0 and $\boldsymbol{\beta}_0$ are computed with Equation 6; the initial training algorithm is exactly the same as that of OS-ELM. Please note that Equation 15 becomes equal to the training algorithm of OS-ELM if $\frac{1}{\alpha_i^2} \mathbf{P}_i$ is replaced with \mathbf{P}_i . Our method provides a forgetting mechanism to OS-ELM with a significantly tiny modification. Moreover, our forgetting mechanism can eliminate the matrix inversion in Equation 15 when batch size = 1 because the size of the target matrix $\mathbf{I} + \mathbf{H}_i \left(\frac{1}{\alpha_i^2} \mathbf{P}_{i-1}\right) \mathbf{H}_i^T$ is $k \times k$ where k denotes the batch size. Therefore, our forgetting mechanism is easily integrated to ONLAD with almost no additional computational cost.

In the past several years, some forgetting mechanisms for OS-ELM have been proposed. Zhao *et al.* firstly studied on a forgetting mechanism for OS-ELM, called FOS-ELM [22] where a sliding-window forgetting approach is adopted. FOS-ELM has a fixed parameter of window size s , where only the latest s training chunks are taken into account. However, this framework requires memory space to store each \mathbf{H} for past s input chunks, which can consume a large amount of hardware resources. λ_{DFF} -OS-ELM [23] enables to adjust variable forgetting factors automatically without any memory for past training data. It also avoids the wind-up phenomenon to maintain stable training with the DFF (Directional Forgetting Factor) method. Although, there is a costly matrix inversion in the DFF algorithm, and it is a challenge for resource-limited devices, the target platforms of our work. On the other hand, our approach can control progress of forgetting with a variable forgetting factor without any costly matrix inversions or memory for past training data.

3.3 Algorithm

ONLAD utilizes OS-ELM of batch size = 1 in conjunction with the proposed forgetting mechanism. The following equations are derived by combining Equation 9 and Equation 15.

$$\begin{aligned}\mathbf{P}_i &= \left(\frac{1}{\alpha_i^2} \mathbf{P}_{i-1}\right) - \frac{\left(\frac{1}{\alpha_i^2} \mathbf{P}_{i-1}\right) \mathbf{h}_i^T \mathbf{h}_i \left(\frac{1}{\alpha_i^2} \mathbf{P}_{i-1}\right)}{1 + \mathbf{h}_i \left(\frac{1}{\alpha_i^2} \mathbf{P}_{i-1}\right) \mathbf{h}_i^T} \\ \boldsymbol{\beta}_i &= \boldsymbol{\beta}_{i-1} + \mathbf{P}_i \mathbf{h}_i^T (\mathbf{t}_i - \mathbf{h}_i \boldsymbol{\beta}_{i-1})\end{aligned}\quad (16)$$

ONLAD is built on an OS-ELM based autoencoder to construct a semi-supervised anomaly detector; $\mathbf{t}_i = \mathbf{x}_i$ holds in Equation 16 because an autoencoder uses input data as target data, too. Finally, the training algorithm of ONLAD is formulated as follows.

$$\begin{aligned}\mathbf{P}_i &= \left(\frac{1}{\alpha_i^2} \mathbf{P}_{i-1}\right) - \frac{\left(\frac{1}{\alpha_i^2} \mathbf{P}_{i-1}\right) \mathbf{h}_i^T \mathbf{h}_i \left(\frac{1}{\alpha_i^2} \mathbf{P}_{i-1}\right)}{1 + \mathbf{h}_i \left(\frac{1}{\alpha_i^2} \mathbf{P}_{i-1}\right) \mathbf{h}_i^T} \\ \boldsymbol{\beta}_i &= \boldsymbol{\beta}_{i-1} + \mathbf{P}_i \mathbf{h}_i^T (\mathbf{x}_i - \mathbf{h}_i \boldsymbol{\beta}_{i-1})\end{aligned}\quad (17)$$

\mathbf{P}_0 and $\boldsymbol{\beta}_0$ are computed as follows (there are no changes from Equation 6).

$$\begin{aligned}\mathbf{P}_0 &= (\mathbf{H}_0^T \mathbf{H}_0)^{-1} \\ \boldsymbol{\beta}_0 &= \mathbf{P}_0 \mathbf{H}_0^T \mathbf{t}_0\end{aligned}\quad (18)$$

The prediction algorithm is formulated as follows.

$$\text{score} = L(\mathbf{x}_i, G(\mathbf{x}_i \cdot \boldsymbol{\alpha} + \mathbf{b})\boldsymbol{\beta}),\quad (19)$$

where L denotes a loss function, and score denotes an anomaly score of \mathbf{x}_i .

3.4 Discussion on Training Stability of OS-ELM

As described in Section 3.1, the computational cost of OS-ELM's training algorithm is significantly reduced by setting batch size to 1 without any deterioration of training results. However, OS-ELM has a concern on its training stability: if $\mathbf{I} + \mathbf{H}_i \mathbf{P}_{i-1} \mathbf{H}_i^T$ in Equation 5 is a singular matrix or close to it, training becomes unstable [13] regardless of batch size. In the context of ONLAD, the problem occurs when $1 + \mathbf{h}_i \mathbf{P}_{i-1} \mathbf{h}_i^T$ in Equation 17 is close to 0. Therefore, ONLAD should stop training when $\epsilon > 1 + \mathbf{h}_i \mathbf{P}_{i-1} \mathbf{h}_i^T$ holds where ϵ denotes a small positive value.

Algorithm 1 An example use case of ONLAD

```

1:  $\alpha \leftarrow \text{random}(), \mathbf{b} \leftarrow \text{random}()$ 
2:  $\mathbf{H}_0 \leftarrow G(\mathbf{x}_0 \cdot \alpha + \mathbf{b}), \mathbf{P}_0 \leftarrow (\mathbf{H}_0^T \mathbf{H}_0)^{-1}, \beta_0 \leftarrow \mathbf{P}_0 \mathbf{H}_0 t_0$ 
3:  $i \leftarrow 1$ 
4: for until  $\{\mathbf{x}_i, \alpha_i\}$  exists do
5:    $\mathbf{h}_i \leftarrow G(\mathbf{x}_i \cdot \alpha + \mathbf{b})$ 
6:   if  $\epsilon > 1 + \mathbf{h}_i \mathbf{P}_{i-1} \mathbf{h}_i^T$  then
7:     print("Singular matrix encountered.")
8:      $i \leftarrow i + 1$ 
9:   continue
10:  end if
11:   $\text{score} \leftarrow L(\mathbf{x}_i, \mathbf{h}_i \beta_{i-1})$ 
12:  if  $\text{score} > \theta$  then
13:    print("Anomaly detected.")
14:  end if
15:   $\mathbf{P}_{i-1} \leftarrow \frac{1}{\alpha_i^2} \mathbf{P}_{i-1}, \mathbf{P}_i \leftarrow \mathbf{P}_{i-1} - \frac{\mathbf{P}_{i-1} \mathbf{h}_i^T \mathbf{h}_i \mathbf{P}_{i-1}}{1 + \mathbf{h}_i \mathbf{P}_{i-1} \mathbf{h}_i^T}, \beta_i \leftarrow \beta_{i-1} + \mathbf{P}_i \mathbf{h}_i^T (\mathbf{x}_i - \mathbf{h}_i \beta_{i-1})$ 
16:   $i \leftarrow i + 1$ 
17: end for

```

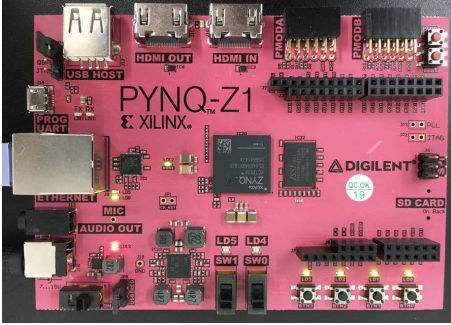


Figure 5: The PYNQ-Z1 board

Table 1: Specification of the PYNQ-Z1 board

Linux Image	PYNQ v2.4 (Ubuntu v18.04)
SoC Chip	Xilinx ZYNQ XC7Z020-1CLG400C CPU: ARM Cortex-A9 650MHz FPGA: Artix-7 FPGA
DRAM	DDR3 512MB
FPGA Resources	
BRAM	280 blocks
DSP	220 slices
FF	106,400 instances
LUT	53,200 instances

3.5 Example Use Case of ONLAD

This section provides a practical example use case of ONLAD (shown in Algorithm 1). α and \mathbf{b} are initialized with random values, then β_0 and \mathbf{P}_0 are computed with Equation 18. At the i th training step in the following loop, firstly the inequality $\epsilon > 1 + \mathbf{h}_i \mathbf{P}_{i-1} \mathbf{h}_i^T$ is evaluated, then the rest of lines are skipped if it is true. In the case of false, then an anomaly score of \mathbf{x}_i is computed with Equation 19. \mathbf{x}_i is judged as an anomaly if the score is greater than a user-defined threshold θ ; otherwise ONLAD judges \mathbf{x}_i as a normal sample. Finally, online training is performed with Equation 17.

4 FPGA Based Implementation of ONLAD Core

This section describes the implementation of ONLAD Core. Here, we implement it on FPGA for fast proof-of-concept. To demonstrate that ONLAD Core can be implemented on resource-limited edge devices, we use the PYNQ-Z1 board (Figure 5) which has a low-cost SoC chip, the Xilinx ZYNQ XC7Z020-1CLG400C chip. Please see Table 1 for the detailed specification of the board. We implement ONLAD Core with Vivado HLS v2018.3 (the clock frequency is 100.0MHz), and the entire on-board system is integrated with Vivado v2018.3.

4.1 Overview of On-board Implementation

Firstly, we provide a brief overview of the on-board implementation. The block diagram is illustrated in Figure 6. The PS (Processing System) part is mainly responsible for preprocessing of input data and controlling the DMA (Direct Memory Access) core. The DMA core converts preprocessed input data in DRAM to AXI4-Stream format data, and transfers them into ONLAD Core. It also converts the outputs (e.g., anomaly scores) of ONLAD Core to AXI4-Memory-Mapped format data, and transfers them back into DRAM. The PL (Programmable Logic) part implements ONLAD Core. ONLAD Core performs sequential learning or prediction according to header information of input packets. After sequential learning is executed, ONLAD Core outputs success signals of training (details are to be explained in Section 4.2.4). It also outputs anomaly scores after prediction is executed.

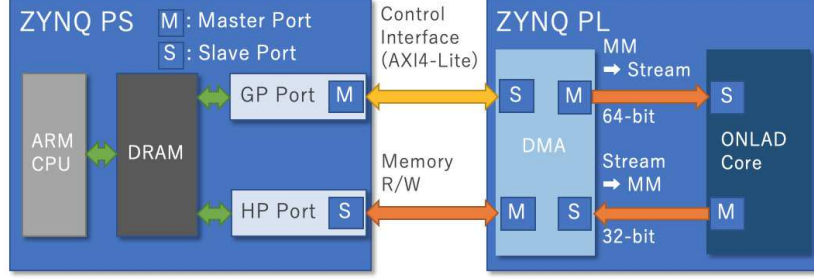


Figure 6: Overview of the on-board implementation

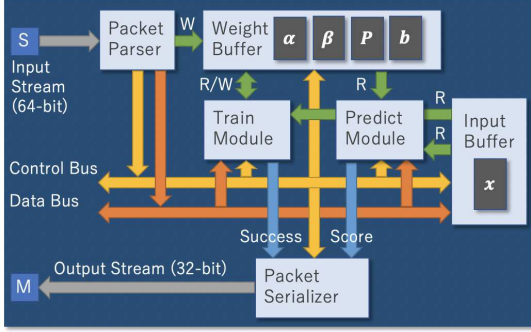


Figure 7: The block diagram of ONLAD Core

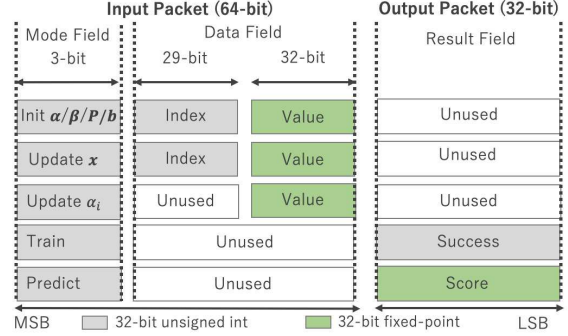


Figure 8: The input/output packet format

4.2 Details of ONLAD Core

This section provides the details of ONLAD Core. Figure 7 illustrates the block diagram. The packet parser parses input packets and controls the other sub-modules according to their header information. Parameters (i.e., α , β , P , b) are managed in the weight buffer implemented with BRAM. The train module and the prediction module are responsible for sequential learning and prediction, respectively. They are implemented mainly with DSP, and designed to use a specific numbers of arithmetic units to save hardware resources. Output results of these two submodules are collected into the packet serializer. The packet serializer creates output packets which embed the output results.

The input/output packet format is detailed in Figure 8. An input packet is of 64-bit length. The first 8-bit field (i.e., Mode Field) indicates which instruction is executed on ONLAD Core. The following 56-bit field (i.e., Data Field) is reserved for several uses depending on each instruction (details are to be explained in the following sections). An output packet is of 32-bit length, and it stores an output result of the train module or the predict module. “Value” and “Score” assume 32-bit fixed point values; all arithmetic operations in both of the train and prediction modules are performed with 32-bit fixed point precision. All the other reserved fields assume 32-bit unsigned integer values.

ONLAD Core is designed to execute the following five instructions: (1) *initialize_parameters*, (2) *create_input_data*, (3) *update_forgetting_factor*, (4) *do_sequential_learning*, and (5) *do_prediction*. The following sections describe how these submodules in ONLAD Core work according to each instruction.

4.2.1 initialize_parameters

This instruction initializes ONLAD Core’s parameters managed in the weight buffer. The packet format is shown in the first row of Figure 8. The target parameter is specified in the mode field of an input packet. “Index” and “Value” in the data field embed an index of the target parameter’s element and its write value. The target parameter is initialized with the following formula.

$$\mathit{target}[\text{Index}] \leftarrow \text{Value} \quad (20)$$

All the parameters are managed as row-major flattened 1-D arrays in the weight buffer.

4.2.2 create_input_data

This instruction updates the values of the input buffer where a single input vector is stored. The input buffer is shared with the train module and the predict module so that they can read an input vector. The packet format (the second row of Figure 8) is almost the same as *initialize_parameters* instruction except for the mode field.

$$\mathit{x}[\text{Index}] \leftarrow \text{Value} \quad (21)$$

An element of the input buffer is updated with the above formula. Please note that n input packets are required in total to fill an n -dimensional input vector.

4.2.3 *update_forgetting_factor*

This instruction updates the forgetting factor α_i managed in the train module. The packet format of this instruction is shown in the third row of Figure 8. “Value” in the data field embeds an update value.

$$\alpha_i \leftarrow \text{Value} \quad (22)$$

α_i is updated with the above formula.

4.2.4 *do_sequential_learning*

This instruction executes sequential learning with the train module. Firstly, the train module reads the latest parameters (i.e., β_{i-1} and P_{i-1}) and an input vector from the weight buffer and the input buffer, respectively. The train module then computes the training algorithm (i.e., Equation 17) and writes the updated parameters back into the weight buffer.

The packet format is shown in the fourth row of Figure 8. An input packet of this instruction is just a trigger for sequential learning. An output packet embeds a success signal which indicates whether the training finished without encountering singular matrices or not (1/0 means encountered/not encountered). As discussed in Section 3.4, $1 + \mathbf{h}_i \mathbf{P}_{i-1} \mathbf{h}_i^T$ in the training algorithm becomes a singular matrix if its value is close to 0, which results in unstable training. In case of encountering singular matrices, the train module interrupts the training, then stops updating parameters to maintain stable training.

4.2.5 *do_prediction*

This instruction executes prediction with the predict module. The predict module reads the latest parameters and an input vector in the same way as the train module. It computes the prediction algorithm (i.e., Equation 19), then outputs an anomaly score.

The packet format is shown in the last row of Figure 8. An input packet of this instruction is also just a trigger for prediction. An output packet embeds an anomaly score computed in the predict module.

5 Evaluation of Anomaly Detection Capability of ONLAD

In this section, anomaly detection capability of ONLAD is evaluated in comparison with BP-NN based models. Specification of the experimental machine is shown in Table 2. All the experiments here are conducted under this machine.

5.1 Experimental Setup

We evaluate the proposed ONLAD in comparison with the following two models: (1) **NN** and (2) **DNN**. NN denotes a 3-layer BP-NN based autoencoder, and DNN denotes a BP-NN based deep autoencoder which consists of five layers in total. All the models including ONLAD run in the experimental machine shown in Table 2, and they are implemented with TensorFlow v1.13.1 [27]. Each of NN and DNN constructs an ONLAD-like model built on a BP-NN based autoencoder instead of an OS-ELM based one.

Toward comprehensive evaluation, two types of testbeds which simulate the (1) **offline environment** and the (2) **online environment** are conducted to compare ONLAD with the other models. We refer to the “offline training environment” as an environment where all the training data and test data are available in advance, and no concept drift is assumed. This is one of most common setups to evaluate semi-supervised anomaly detection models. The purpose of the testbed is to measure fundamental generalization capability of ONLAD in comparison with the other models. Please note that

Table 2: Specification of the experimental machine

OS	Ubuntu 18.04
CPU	Intel Core i7 6700 3.4GHz
GPU	Nvidia GTX 1070 8GB
DRAM	DDR4 16GB
Storage	SSD 512GB

Table 3: The datasets

Name	Samples	Features	Classes
Fashion MNIST [24]	70,000	784	10
MNIST [25]	70,000	784	10
Smartphone HAR [26]	5,744	561	6
Drive Diagnosis [26]	58,509	48	11
Letter Recognition [26]	20,000	16	26

Table 4: The search ranges of hyperparameters

	ONLAD		NN		DNN
G_{hidden}	{Sigmoid [28], Identity ⁴ }	G_{hidden}	{Sigmoid, Relu [29]}	G_{hidden}	{Sigmoid, Relu}
$p(x)$	Uniform ⁵	G_{out}	Sigmoid	G_{out}	Sigmoid
\tilde{N}_i	$\{2^n n = 1, 2, \dots, 10\}$	\tilde{N}_1	$\{2^n n = 1, 2, \dots, 10\}$	$\tilde{N}_1, \tilde{N}_2, \tilde{N}_3$	$\{2^n n = 1, 2, \dots, 10\}$
L	MSE ⁶	L	MSE	L	MSE
α_i	{0.95, 0.96, ..., 1.00}	O	{SGD[30], Adam[31]}	O	{SGD, Adam}
		B	32	B	32
		E	10	E	20

the testbed does not evaluate effectiveness of ONLAD’s forgetting mechanism (i.e., α_i is always set to 1.00) because there is no need to perform forgetting as no concept drift is assumed.

On the other hand, we refer to the “online environment” as an environment where at first only a small part of a dataset is given, and the rest of the dataset will sequentially arrive. It is also assumed that concept drift occurs in this environment in contrast to the offline environment. The purpose of the testbed is to evaluate robustness against concept drift. We show effectiveness of the forgetting mechanism of ONLAD here. In the rest of this paper, the above two testbeds are referred as the **offline testbed** and the **online testbed**, respectively.

Open classification datasets listed in Table 3 are used to construct both of the testbeds. All the data samples’ values are normalized within $[0, 1]$ with minmax normalization. Hyperparameters of each model are explored within the ranges detailed in Table 4³.

5.2 Experimental Method

This section describes the experimental methods of the offline testbed and the online testbed, respectively.

Algorithm 2 shows the experimental method of the offline testbed. In this testbed, each dataset is divided into training samples \mathbf{X}_{train} (80%) and test samples \mathbf{X}_{test} (20%) in advance. Suppose we have a dataset which consists of c classes in total. Let training/test samples of class i be normal training/test samples $\mathbf{X}_{normal_train}/\mathbf{X}_{normal_test}$, then test samples of class $j \neq i$ be anomalies $\mathbf{X}_{anomaly}$. The number of anomalies is limited to 10 percent of that of the normal test samples to simulate a practical situation; anomalies are the minority in most cases. Each model is trained with normal training samples, and evaluated with a test set which contains normal test samples and anomalies $[\mathbf{X}_{normal_test}, \mathbf{X}_{anomaly}]$. Regarding to evaluation metrics, we use AUC (Area Under Curve) to measure anomaly detection capability of each model. AUC is one of the most widely used metrics to evaluate accuracy of anomaly detection models independently of particular anomaly score thresholds. The above whole process is repeated until $i < c$, after that all the AUC scores are averaged. The output score is recorded as a result of a single trial; the final AUC scores reported in Table 5 are further averaged over 20 trials. 5-fold cross validation with training samples is used for hyperparameter tuning.

Algorithm 3 also describes the experimental method of the online testbed. In this testbed, each dataset is divided into initial samples \mathbf{X}_{init} (10%), test samples \mathbf{X}_{test} (45%), and validation samples \mathbf{X}_{valid} (45%), respectively. Initial samples represent data samples which users have prepared in advance. They are used to train each model as initialization. On the other hand, test samples and validation samples represent for data samples which arrive sequentially in time-series. They are used to evaluate whether each model can correctly detect anomalies among data serieses where concept drift occurs. Especially, test samples are used to measure the final AUC scores, while validation samples are only for hyperparameter tuning. Algorithm 3 shows the case of using test samples. Firstly, test samples are randomly split into normal samples \mathbf{X}_{normal} (90%) and anomalies $\mathbf{X}_{anomaly}$ (10%). Then, a list which contains integer numbers from 0 to $c - 1$ is constructed, and is randomly shuffled. The output number sequence represents the transition of the normal class; suppose $indices = [2, 0, 1]$, the normal class is changing to 2, 0, and 1 in this order at each concept. We equally assign anomalies of different classes from the normal class into each concept (the entire data series is denoted as \mathbf{X}_{online}). Each model is trained with initial samples of the first normal class $\mathbf{X}_{init}^{(indices[0])}$. Then, each model computes an anomaly score for each incoming data sample given from \mathbf{X}_{online} , then sequentially learns

³ G_{hidden} : an activation function applied to all the hidden layers in common. G_{out} an activation function applied to the output layer. $p(x)$: a probability density function used for random initialization of ONLAD’s parameters. \tilde{N}_i : the number of nodes of the i th hidden layer. L : a loss function. α_i : the forgetting factor of ONLAD. O : an optimization algorithm. B : batch size. E : the number of training epochs.

⁴ $G(\mathbf{x}) = \mathbf{x}$

⁵ $p(x) = \frac{1}{2}$ if $(-1 \leq x \leq 1)$ else 0

⁶ $L(\mathbf{x}, \mathbf{y}) = \frac{1}{n} \sum_{i=0}^n (x_i - y_i)^2$

Algorithm 2 The experimental method of the offline testbed

```

1:  $\mathbf{X}_{train} \equiv [\mathbf{X}_{train}^{(0)}, \mathbf{X}_{train}^{(1)}, \dots, \mathbf{X}_{train}^{(c-1)}], \mathbf{X}_{test} \equiv [\mathbf{X}_{test}^{(0)}, \mathbf{X}_{test}^{(1)}, \dots, \mathbf{X}_{test}^{(c-1)}]$ 
2:  $average\_auc \leftarrow 0$ 
3: for  $i \leftarrow 0$  to  $c - 1$  do
4:    $\mathbf{X}_{normal\_train} \leftarrow \mathbf{X}_{train}^{(i)}, \mathbf{X}_{normal\_test} \leftarrow \mathbf{X}_{test}^{(i)}$ 
5:    $\mathbf{X}_{anomaly} \leftarrow \mathbf{X}_{test}^{(j \neq i)}$ 
6:    $\mathbf{X}_{anomaly} \leftarrow random\_sample(\mathbf{X}_{anomaly}, len(\mathbf{X}_{normal\_test}) \times 0.1)$ 
7:    $model.train(\mathbf{X}_{normal\_train})$ 
8:    $scores \leftarrow model.predict([\mathbf{X}_{normal\_test}, \mathbf{X}_{anomaly}])$ 
9:    $average\_auc \leftarrow average\_auc + calc\_auc(scores)$ 
10:   $model.reset()$ 
11: end for
12:  $average\_auc \leftarrow \frac{average\_auc}{c}$ 

```

Algorithm 3 The experimental method of the online testbed

```

1:  $\mathbf{X}_{init} \equiv [\mathbf{X}_{init}^{(0)}, \mathbf{X}_{init}^{(1)}, \dots, \mathbf{X}_{init}^{(c-1)}], \mathbf{X}_{test} \equiv [\mathbf{X}_{test}^{(0)}, \mathbf{X}_{test}^{(1)}, \dots, \mathbf{X}_{test}^{(c-1)}]$ 
2:  $\mathbf{X}_{normal}, \mathbf{X}_{anomaly} \leftarrow random\_split(\mathbf{X}_{test}, "9 : 1")$ 
3:  $indices \leftarrow [0, 1, \dots, c - 1]$ 
4:  $random\_shuffle(indices)$ 
5:  $\mathbf{X}_{online} \leftarrow [\mathbf{X}_{online}^{(0)} \equiv [\mathbf{X}_{normal}^{(0)}, \mathbf{X}_{anomaly}^{(j \neq 0)}], \dots, \mathbf{X}_{online}^{(c-1)} \equiv [\mathbf{X}_{normal}^{(c-1)}, \mathbf{X}_{anomaly}^{(j \neq c-1)}]]$ 
6:  $model.train(\mathbf{X}_{init}^{(indices[0])})$ 
7:  $scores \leftarrow []$ 
8: for  $i \leftarrow 0$  to  $c - 1$  do
9:    $random\_shuffle(\mathbf{X}_{online}^{(indices[i])})$ 
10:  for all  $\mathbf{x} \in \mathbf{X}_{online}^{(indices[i])}$  do
11:     $score \leftarrow model.predict(\mathbf{x})$ 
12:     $scores.append(score)$ 
13:   $model.train(\mathbf{x})$ 
14:  end for
15: end for
16:  $auc \leftarrow calc\_auc(scores)$ 

```

it. Finally, an AUC score is calculated with the output anomaly scores, and it is recorded as a result of a single trial. The final AUC scores reported in Table 6 are averaged over 20 trials as with the offline testbed.

5.3 Experimental Results

The experimental results of the offline testbed is shown in Table 5. The hyperparameter settings are also detailed in Table 7. As shown in Table 5, NN and DNN get slightly higher AUC scores than ONLAD by roughly from 0.01 up to 0.03 point for almost all the datasets in the offline testbed. This result implies that BP-NN based autoencoders have slightly higher generalization capability than OS-ELM based ones in the context of semi-supervised anomaly detection. However, NN and DNN are iteratively trained for many epochs (10 and 20 epochs, respectively) to achieve their best generalization capability. ONLAD in contrast is always able to compute the optimal output weight only in one epoch. It is also observed that ONLAD gets its best AUC scores with smaller or equal model size (i.e., the number of hidden nodes) in comparison with NN and DNN for all the datasets as shown in Table 7. That helps to save hardware resources, and moreover significantly reduce the computational cost of the training algorithm (the cost is proportional to the square of the number of hidden nodes as shown in Equation 8). This advantage allows ONLAD Core to run on resource-limited edge devices. In summary, ONLAD gets comparable generalization capability to the BP-NN based models in much smaller number of training epochs with smaller or equal model size.

The experimental results of the online testbed is shown in Table 6. The hyperparameter settings are also detailed in Table 8. Here, we provide another model to discuss on effectiveness of ONLAD’s forgetting mechanism: ONLAD-NF (ONLAD-No-Forgetting-mechanism) shown in Table 6 represents a special case of ONLAD which disables the forgetting mechanism by fixing α_i to 1.00. The hyperparameter settings of ONLAD-NF are exactly the same as ONLAD except for α_i . As shown in Table 6, ONLAD-NF gets significantly lower AUC scores than ONLAD by approximately from 0.2 up to 0.3 point. The reason is quite obvious; ONLAD-NF does not have any functionalities to forget past learned samples, therefore it gradually becomes more difficult to detect anomalies every time the normal class changes. NN and DNN, on the other hand, achieve higher AUC scores than ONLAD-NF because BP-NNs have the catastrophic forgetting nature [32], and it works as an implicit forgetting mechanism. It allows the NN based

Table 5: AUC scores in the offline testbed

Dataset	ONLAD	NN	DNN
Fashion MNIST	0.906	0.919	0.915
MNIST	0.941	0.957	0.960
Smartphone HAR	0.912	0.882	0.890
Drive Diagnosis	0.939	0.954	0.974
Letter Recognition	0.954	0.958	0.985

Table 6: AUC scores in the online testbed

Dataset	ONLAD-NF	ONLAD	NN	DNN
Fashion MNIST	0.573	0.865	0.678	0.687
MNIST	0.593	0.890	0.657	0.721
Smartphone HAR	0.566	0.778	0.789	0.767
Drive Diagnosis	0.555	0.782	0.732	0.804
Letter Recognition	0.552	0.867	0.730	0.789

Table 7: The hyperparameter settings in the offline testbed

Dataset	ONLAD $\{G_{hidden}, p(x), \tilde{N}_1\},$ $\{L, \alpha_i\}$	NN $\{G_{hidden}, G_{out}, \tilde{N}_1\},$ $\{L, O, B, E\}$	DNN $\{G_{hidden}, G_{out}, \tilde{N}_1, \tilde{N}_2, \tilde{N}_3\},$ $\{L, O, B, E\}$
Fashion MNIST	{Identity, Uniform, 64}, {MSE, 1.00}	{Relu, Sigmoid, 64}, {MSE, Adam, 32, 10}	{Relu, Sigmoid, 64, 32, 64}, {MSE, Adam, 32, 20}
MNIST	{Identity, Uniform, 64}, {MSE, 1.00}	{Relu, Sigmoid, 64}, {MSE, Adam, 32, 10}	{Relu, Sigmoid, 64, 32, 64}, {MSE, Adam, 32, 20}
Smartphone HAR	{Identity, Uniform, 128}, {MSE, 1.00}	{Relu, Sigmoid, 1,024}, {MSE, Adam, 32, 10}	{Relu, Sigmoid, 512, 1,024, 512}, {MSE, Adam, 32, 20}
Drive Diagnosis	{Sigmoid, Uniform, 16}, {MSE, 1.00}	{Relu, Sigmoid, 512}, {MSE, Adam, 32, 10}	{Relu, Sigmoid, 512, 1,024, 512}, {MSE, Adam, 32, 20}
Letter Recognition	{Sigmoid, Uniform, 8}, {MSE, 1.00}	{Relu, Sigmoid, 1,024}, {MSE, Adam, 32, 10}	{Relu, Sigmoid, 512, 1,024, 512}, {MSE, Adam, 32, 20}

Table 8: The hyperparameter settings in the online testbed

Dataset	ONLAD $\{G_{hidden}, p(x), \tilde{N}_1\},$ $\{L, \alpha_i\}$	NN $\{G_{hidden}, G_{out}, \tilde{N}_1\},$ $\{L, O, B, E\}$	DNN $\{G_{hidden}, G_{out}, \tilde{N}_1, \tilde{N}_2, \tilde{N}_3\},$ $\{L, O, B, E\}$
Fashion MNIST	{Sigmoid, Uniform, 64}, {MSE, 0.99}	{Relu, Sigmoid, 64}, {MSE, Adam, 32, 10}	{Relu, Sigmoid, 64, 32, 64}, {MSE, Adam, 32, 20}
MNIST	{Sigmoid, Uniform, 64}, {MSE, 0.99}	{Relu, Sigmoid, 64}, {MSE, Adam, 32, 10}	{Relu, Sigmoid, 64, 32, 64}, {MSE, Adam, 32, 20}
Smartphone HAR	{Identity, Uniform, 16}, {MSE, 0.97}	{Sigmoid, Sigmoid, 32}, {MSE, Adam, 32, 10}	{Sigmoid, Sigmoid, 32, 2, 32}, {MSE, Adam, 32, 20}
Drive Diagnosis	{Sigmoid, Uniform, 16}, {MSE, 0.99}	{Sigmoid, Sigmoid, 16}, {MSE, Adam, 32, 10}	{Sigmoid, Sigmoid, 16, 8, 16}, {MSE, Adam, 32, 20}
Letter Recognition	{Sigmoid, Uniform, 8}, {MSE, 0.95}	{Relu, Sigmoid, 16}, {MSE, Adam, 32, 10}	{Relu, Sigmoid, 16, 8, 16}, {MSE, Adam, 32, 20}

Table 9: The hyperparameter settings in Section 6

ONLAD Core $\{G_{hidden}, L\}$	NN-CPU and NN-GPU $\{G_{hidden}, G_{out}, L, O, B\}$	DNN-CPU and DNN-GPU $\{G_{hidden}, G_{out}, L, O, B\}$
{Identity, MSE}	{Relu, Sigmoid, MSE, Adam, 1}	{Relu, Sigmoid, MSE, Adam, 1}

models to forget past learned samples and address concept drift to some extent. However, BP-NNs do not have any numerical parameters to analytically control the forgetting mechanism unlike ONLAD. Hence, it is a reasonable result that our ONLAD stably gets favorable AUC scores over the others; ONLAD gets much higher AUC scores than NN and DNN by roughly from 0.08 up to 0.23 point for three datasets out of five ones, and also our model did not even get the worst AUC scores for the rest two datasets.

6 Evaluation of Hardware Performance of ONLAD Core

In this section, the FPGA based ONLAD Core is evaluated in terms of training/prediction latency, resource utilization, and on-board power consumption.

6.1 Experimental Setup

We compare ONLAD Core with the following software implementations: (1) NN-CPU, (2) DNN-CPU, (3) NN-GPU, and (4) DNN-GPU. These are virtually the same as NN and DNN used in Section 5, though they are executed with specific devices; {*}-CPU runs only with CPU while {*}-GPU runs with GPU in addition to CPU. All of the implementations are developed with Tensorflow v1.13.1 as with NN and DNN used in Section 5. The library is built

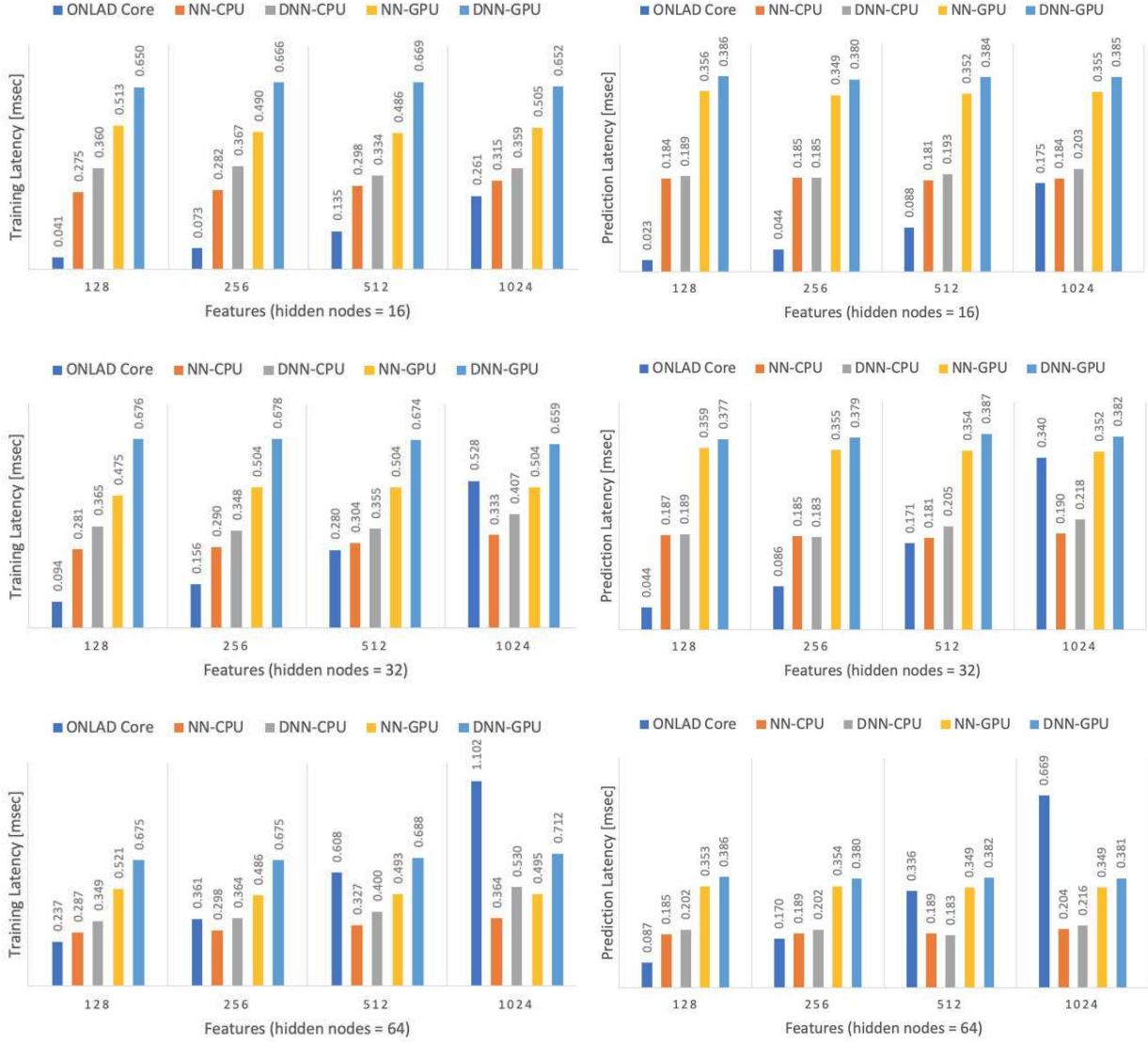


Figure 9: Comparison of training latency (the left side) and prediction latency (the right side)

with AVX2 (Advanced Vector Extensions 2) instructions and -O3 option to accelerate the software implementations. It is also built with CUDA [33] v10.0 for GPGPU execution.

The hyperparameter setting of each implementation is detailed in Table 9. $p(x)$, α_i , and E are removed from the table because these parameters are irrelevant to the evaluation metrics (i.e., training/prediction latency, resource utilization, and on-board power consumption). As shown in the table, batch size of NN- $\{*\}$ and DNN- $\{*\}$ is set to 1 for fair comparison of training/prediction latency; ONLAD Core’s batch size is fixed to 1 originally.

6.2 Latency

In this section, ONLAD Core is compared with the others in terms of training/prediction latency. Here, “training latency” means the elapsed time from receiving an input sample until training is finished. On the other hand, “prediction latency” means the elapsed time from receiving an input sample until an anomaly score is computed.

The experimental results are shown in Figure 9. Every reported latency time is averaged over 50,000 trials. The left side of the figure shows training latency times, while the right side shows prediction latency times. Each subfigure shows latency times of the common number of hidden nodes with varying input features (i.e., the number of input nodes).

Table 10: FPGA resource utilization of ONLAD module

Hidden Nodes = 16				
Features	BRAM [%]	DSP [%]	FF [%]	LUT [%]
128	10.0	40.0	16.0	29.9
256	12.9	40.0	16.1	30.0
512	18.6	40.0	16.1	30.0
1,024	30.0	40.0	16.1	30.0
Hidden Nodes = 32				
Features	BRAM [%]	DSP [%]	FF [%]	LUT [%]
128	13.6	40.0	16.0	29.9
256	19.3	40.0	16.0	30.0
512	30.7	40.0	16.0	30.0
1,024	53.6	40.0	16.0	30.0
Hidden Nodes = 64				
Features	BRAM [%]	DSP [%]	FF [%]	LUT [%]
128	24.3	40.0	15.9	30.0
256	35.7	40.0	15.9	30.0
512	58.6	40.0	16.0	30.0
1,024	104.2	40.0	16.0	30.1

Table 12: FPGA resource utilization of the on-board implementation

BRAM [%]	DSP [%]	FF [%]	LUT [%]
55.4	32.7	11.6	25.8

Table 11: The size of each parameter

Parameter	Size
α	$n \times \tilde{N}$
β	$\tilde{N} \times m$
P	$\tilde{N} \times \tilde{N}$
b	\tilde{N}

In this experiment, training latency of ONLAD Core is faster than that of NN-CPU, DNN-CPU, NN-GPU, and DNN-GPU by x1.95, x2.45, x3.38, and x4.51 in average. Prediction latency of ONLAD Core is also faster than that of the software implementations by x2.29, x2.37, x4.38, and x4.73 in average. As shown in the figure, reported times of all the software implementations are almost constant even when the number of input features is increased, in other words, all the software implementations suffer from software overheads (i.e., function calls and memory allocation). NN-GPU and DNN-GPU are especially slow because of the communication cost between GPU and CPU in addition to the software overheads. For these reasons, ONLAD Core is much faster in the range of small input features; otherwise it becomes slower than the others vice versa because the computational cost of the ONLAD Core’s training/prediction algorithm is proportional to the number of input features. It is also a notable fact that the computational cost of the training algorithm is proportional to the square of the number of hidden nodes. However, ONLAD gets favorable anomaly detection capability with much smaller numbers of hidden nodes than those of input features as observed in Section 5.3, which indirectly suppresses the computational cost of ONLAD Core.

6.3 FPGA Resource Utilization

This section evaluates FPGA resource utilization of ONLAD Core with varying the numbers of input features and hidden nodes. Pre-synthesis resource utilization reports produced by Vivado HLS are used as results.

The experimental results are shown in Table 11. It is reasonable that the utilizations of DSP, FF, and LUT are almost constant regardless of input features and hidden nodes, because the train/predict module of ONLAD Core is designed to use a specific number of arithmetic units as mentioned in Section 4.2. Therefore, all we have to care is the utilization of BRAM. As shown in the table, more BRAM instances are consumed as the numbers of input features and hidden nodes are increased. This result is consistent with the fact that the weight buffer which stores the parameters (i.e., α , β , P , b) is implemented with BRAM. Table 10 shows the size of each parameter. n , \tilde{N} , and m denote the numbers of input nodes, hidden nodes, and output nodes, respectively. The table shows that the space complexity is proportional to the square of \tilde{N} . However, as mentioned in the previous section, ONLAD can obtain favorable anomaly detection capability with small \tilde{N} , which helps ONLAD Core to save BRAM instances. As a result, all the resource utilizations of ONLAD Core is under the limit except for the largest setting $(n, \tilde{N}) = (1024, 64)$.

6.4 Power Consumption of On-board Implementation

In this section, we compare the on-board implementation with the others in terms of power consumption during the **idle state** and the **busy state**. Here, “idle state” means the state where only bitstream is written to the board and no instructions are issued. On the other hand, “busy state” means the state where the system iteratively executes sequential training with input samples randomly generated. Power consumption of the on-board implementation is measured with a common watt meter, and the other software implementations’ are with s-tui [34] and nvidia-smi

Table 13: Comparison of power consumption

	Our On-board Implementation [W]	NN-CPU [W]	DNN-CPU [W]	NN-GPU [W]	DNN-GPU [W]
Idle State	2.5	4.9	4.9	15.9 CPU: 4.9 GPU: 11.0	15.9 CPU: 4.9 GPU: 11.0
Busy State	2.9	19.5	23.2	77.6 CPU: 15.6 GPU: 62.0	78.6 CPU: 15.6 GPU: 63.0

command. We use s-tui, a terminal based CPU stress and monitoring tool, for measurement of power consumption of CPU, while nvidia-smi command provided by NVIDIA is for that of GPU. For fair comparison, the numbers of hidden nodes and input features are set to 32 and 1,024 for all the implementations in common. Table 12 shows the resource utilization of the on-board implementation reported by Vivado.

Table 13 shows the experimental results. It is observed that the on-board implementation actually works at 2.5 W during the idle state, and at 2.9 W during the busy state. Comparing with the others, our on-board implementation works at lower power consumption from x2.0 up to x6.4 during the idle state and from x6.7 up to x27.1 during the busy state. Please note that the reported power consumptions of our on-board implementation contain not only those of ONLAD Core but also those of the ARM Cortex-A9 processor; the power consumptions of ONLAD Core itself are even less than the reported numbers.

7 Conclusions

In this work, we proposed an ON-device sequential Learning semi-supervised Anomaly Detector called ONLAD. We also proposed an IP core of ONLAD, called ONLAD Core. The proposed algorithm was designed to address concept drift, time-series changes of distributions of normal data, with an adaptively controllable forgetting factor. ONLAD Core also realized a low-cost on-device learning on resource-limited edge devices, which enables standalone execution where no data transfer between external server machines and edge devices is assumed. That helps to avoid a potential risk to cause data breaches which threaten data security.

Experimental results using open datasets showed that our ONLAD has comparable generalization capability to BP-NN based models. It was also found that ONLAD has favorable anomaly detection capability especially in an environment which simulates concept drift. Experimental results on hardware performance of our FPGA-based ONLAD Core showed that its training latency and prediction latency are faster than BP-NN based software implementations by x1.95 - x4.51 and x2.29 - x4.73, respectively. It was also confirmed that our on-board implementation of ONLAD Core actually works at x2.0 - x6.4 lower power consumption during the idle state, and x6.7 - x27.1 lower power consumption during the busy state in comparison with the other software implementations.

References

- [1] V. Cahndola, A. Banerjee, and V. Kumar. Anomaly Detection: A Survey. *ACM Computing Surveys*, 41(3):1–58, Jul 2009.
- [2] D.A. Reynolds. *Encyclopedia of biometrics*, pages 659–663. Springer US, 2009.
- [3] T. Cover and P. Hart. Nearest neighbor pattern classification. *IEEE Transactions on Information Theory*, 13(1):21–27, Jan 1967.
- [4] S. Wold, K. Esbensen, and P. Geladi. Principal component analysis. *Chemometrics and Intelligent Laboratory Systems*, 2(1-3):37–52, Aug 1987.
- [5] Y. Chen, X.S. Zhou, and T.S. Huang. One-class SVM for learning in image retrieval. In *Proceedings of the IEEE International Conference on Image Processing*, pages 34–37, Oct 2001.
- [6] S.M. Erfani, S. Rajasegarar, S. Karunasekera, and C. Leckie. High-dimensional and large-scale anomaly detection using a linear one-class SVM with deep learning. *Pattern Recognition*, 58:121–134, Oct 2016.
- [7] M. Sakurada and T. Yairi. Anomaly Detection Using Autoencoders with Nonlinear Dimensionality Reduction. In *Proceedings of the Workshop on Machine Learning for Sensory Data Analysis*, pages 4–11, Jul 2014.
- [8] T. Schlegl, P. Seeböck, S.M. Waldstein, U.S. Erfurth, and G. Langs. Unsupervised Anomaly Detection with Generative Adversarial Networks to Guide Marker Discovery. In *Proceedings of the International Conference on Information Processing in Medical Imaging*, pages 146–157, May 2017.

- [9] I. Žliobaitė, M. Pechenizkiy, and J. Gama. An overview of concept drift adaptation. *ACM Computing Surveys*, 46(4):44:1–44:37, Apr 2014.
- [10] G.I. Webb, M.J. Pazzani, and D. Billsus. Machine Learning for User Modeling. *User Modeling and User-Adapted Interaction*, 11(1-2):19–29, Mar 2001.
- [11] M. Hind, S. Mehta, A. Mojsilovic, R. Nair, K.N. Ramamurthy, A. Olteanu, and K.R. Varshney. Increasing Trust in AI Services through Supplier’s Declarations of Conformity. *CoRR*, abs/1808.07261, 2018.
- [12] M. Tsukada, M. Kondo, and H. Matsutani. OS-ELM-FPGA: An FPGA-Based Online Sequential Unsupervised Anomaly Detector. In *Proceedings of the International European Conference on Parallel and Distributed Computing (Euro-Par) Workshops*, pages 518–529, Dec 2018.
- [13] N.Y. Liang, G.B. Huang, P. Saratchandran, and N. Sundararajan. A Fast and Accurate Online Sequential Learning Algorithm for Feedforward Networks. *IEEE Transactions on Neural Networks*, 17(6):1411–1423, Nov 2006.
- [14] G. Hinton and R. Salakhutdinov. Reducing the Dimensionality of Data with Neural Networks. *Science*, 313(5786):504–507, Jul 2006.
- [15] G.B. Huang, Q.Y. Zhu, and C.K. Siew. Extreme Learning Machine: A New Learning Scheme of Feedforward Neural Networks. In *Proceedings of the International Joint Conference on Neural Networks*, pages 985–990, Jul 2004.
- [16] G.H. Golub and C. Reinsch. Singular value decomposition and least squares solutions. *Numerische Mathematik*, 14(5):403–420, Apr 1970.
- [17] P. Vincent, H. Larochelle, Y. Bengio, and P.A. Manzagol. Extracting and composing robust features with denoising autoencoders. In *Proceedings of the International Conference on Machine Learning*, pages 1096–1103, Jul 2008.
- [18] A. Jinwon and C. Sungzoon. Variational autoencoder based anomaly detection using reconstruction probability. *Special Lecture on IE*, 2:1–18, 2013.
- [19] Q. Wang et al. Kernel Principal Component Analysis. In *Proceedings of the International Conference on Artificial Neural Networks*, pages 583–588, Jun 1997.
- [20] D. Liu, Y. Wu, and H. Jiang. FP-ELM: An online sequential learning algorithm for dealing with concept drift. *Neurocomputing*, 207(26):322–334, Sep 2016.
- [21] G.H. Golub and C.F.V Loan. *Matrix Computations*. Johns Hopkins University Press, 3rd edition, Oct 1996.
- [22] J. Zhao, Z. Wang, and D.S Park. Online sequential extreme learning machine with forgetting mechanism. *Neurocomputing*, 87(15):79–89, Jun 2012.
- [23] S.G. Soares and R. Araújo. An adaptive ensemble of on-line Extreme Learning Machines with variable forgetting factor for dynamic system prediction. *Neurocomputing*, 171(1):693–707, Jan 2016.
- [24] H. Xiao, K. Rasul, and R. Vollgraf. Fashion-MNIST: a Novel Image Dataset for Benchmarking Machine Learning Algorithms. <https://github.com/zalando-research/fashion-mnist>, 2017.
- [25] Y. Lecun and C. Cortes. MNIST handwritten digit database. <http://yann.lecun.com/exdb/mnist/>, 2010.
- [26] D. Dua and C. Graff". UCI Machine Learning Repository, 2017.
- [27] M. Abadi et al. TensorFlow: Large-Scale Machine Learning on Heterogeneous Systems. In *Proceedings of the USENIX Conference on Operating Systems Design and Implementation*, pages 265–283, March 2016.
- [28] G. Cybenko. Approximation by Superpositions of a Sigmoidal Function. *Mathematics of Control, Signals and Systems*, 2(4):303–314, Dec 1989.
- [29] V. Nair and G. Hinton. Rectified Linear Units Improve Restricted Boltzmann Machines. In *Proceedings of the International Conference on Machine Learning*, pages 807–814, Jun 2010.
- [30] H. Robbins and S. Monro. A Stochastic Approximation Method. *The Annals of Mathematical Statistics*, 22(3):400–407, Sep 1951.
- [31] D.P. Kingma and J. Ba. Adam: A Method for Stochastic Optimization. *CoRR*, abs/1412.6980, Jan 2014.
- [32] M. McCloskey and N.J Cohen. Catastrophic Interference in Connectionist Networks: The Sequential Learning Problem. *Psychology of Learning and Motivation*, 24:109–165, 1989.
- [33] J. Nickolls, I. Buck, M. Garland, and K. Skadron. Scalable Parallel Programming with CUDA. *ACM Queue*, 6(2):40–53, Apr 2008.
- [34] A. Manuskin. Terminal-based CPU stress and monitoring utility. <https://github.com/amanusk/s-tui>, 2017.